

# Degradation of selected industrial dyes using Mg-doped TiO<sub>2</sub> polyscales under natural sun light as an alternative driving energy

H. P. Shivaraju<sup>1,2</sup> · G. Midhun<sup>1</sup> · K. M. Anil Kumar<sup>1</sup> · S. Pallavi<sup>1</sup> ·  
N. Pallavi<sup>1</sup> · Shahmoradi Behzad<sup>3</sup>

Received: 27 September 2016 / Accepted: 21 February 2017 / Published online: 21 March 2017  
© The Author(s) 2017. This article is an open access publication

**Abstract** Designing photocatalytic materials with modified functionalities for the utilization of renewable energy sources as an alternative driving energy has attracted much attention in the area of sustainable wastewater treatment applications. Catalyst-assisted advanced oxidation process is an emerging treatment technology for organic pollutants and toxicants in industrial wastewater. Preparation of visible-light-responsive photocatalyst such as Mg-doped TiO<sub>2</sub> polyscales was carried out under mild sol–gel technique. Mg-doped TiO<sub>2</sub> polyscales were characterized by powder XRD, SEM, FTIR, and optical and photocatalytic activity techniques. The Mg-doped TiO<sub>2</sub> showed a mixed phase of anatase and rutile with an excellent crystallinity, structural elucidations, polyscales morphology, consequent shifting of bandgap energy and adequate photocatalytic activities under visible range of light. Mg-doped TiO<sub>2</sub> polyscales were investigated for their efficiencies in the degradation of most commonly used industrial dyes in the real-time textile wastewater. Mg-doped TiO<sub>2</sub> polyscales showed excellent photocatalytic degradation efficiency in both model

industrial dyes (65–95%) and textile wastewater (92%) under natural sunlight as an alternative and renewable driving energy.

**Keywords** Sol–gel · Photocatalyst · TiO<sub>2</sub> polyscales · Organic dyes · Textile wastewater · Natural sunlight · Alternative driving energy

## Introduction

Water is one of the precious resources that cannot be replaced by man for his daily commodities, development, and industrialization. With increased industrialization and enormous population growth, the quality of water across the world is decreasing owing to exploitation (Qu et al. 2013). Along with other resources, water is an unavoidable raw material for most of the industries. The wastewater generation rate in India is roughly 36,000 million l/day and millions of gallons of wastewater are produced by the industries (CPCB 2009). Potential treatment of wastewater at industrial level is one of the sustainable ways to protect water resource and to minimize the pollution level caused by them. Textile mills, food and dairy, printing and paper, pharmaceutical, and paint industries are the major consumers of large amount of water and the largest industrial sectors causing intense water pollution. Wastewater disposed by these industries is mostly contaminated with a large variety of synthetic organic dyes and pigments (Divya et al. 2013; Wang et al. 2015; Blanco et al. 2012). Moreover, usage of such colorants in these industries is unavoidable nowadays. The availability of a variety of colored food and drugs, cloths, papers, and dye combination that are available in today's markets make the statement valid. More than 10,000 dyes variants are

**Electronic supplementary material** The online version of this article (doi:10.1007/s13201-017-0546-0) contains supplementary material, which is available to authorized users.

✉ H. P. Shivaraju  
shivarajuenvi@gmail.com

- <sup>1</sup> Department of Water and Health, Faculty of Life Sciences, JSS University, Mysore 570015, India
- <sup>2</sup> Center for Water, Food and Energy, GREENS Trust, Harikaranahalli, Dombarahalli Post, Turuvekere Taluka, Tumkur District, Karnataka, India 572215
- <sup>3</sup> Environmental Health Research Center, Kurdistan University of Medical Sciences, Sanandaj, Iran

commercially available in the market and more than 0.7 million tons of dyes and color variants are produced annually across the world (Zolinger 1987; Saggiaro et al. 2011; Maleki and Shahmoradi 2012; Behzad et al. 2012). The textile and food industries are the largest consumers of dye and colorant stuffs in the world; a large percentage of the synthetic dyes and pigments is washed off during the coloration process that results in the development of colored wastewater (Dave and Dave 2009; Divya et al. 2009; Wijannarong et al. 2013; Gupta et al. 2014; Weber and Adams 1995). Discharge of a colored wastewater with a small quantity of dyes and pigments leads to the development of color in the whole aquatic system and causes severe environmental risks (Hassani et al. 2008; Mohamed et al. 2012). The non-biodegradable nature of these dyes and colorants in the aqueous system causes a serious environmental hazard by impacting on evaporation rate, dissolution, precipitation, and biological activities (Nordin et al. 2013; Polak et al. 2016). The organic dyes in wastewater and natural water bodies are aesthetically unpleasant; they hinder the oxygenation ability and disturb the aquatic ecosystem by impact on food chain (Firmino et al. 2010; Khataee et al. 2013). Many conventional treatment methods are available for the treatment of industrial wastewater but they are unable in complete removal of such dyes and pigments from wastewater. Some advanced treatment techniques like adsorption and membrane filtration are used for the treatment of wastewater but these techniques are relied on the production of secondary pollutants and ecologically not viable methods. In addition, these techniques are not economic, difficult to handle, and not a sustainable way to treat industrial wastewater. Hence, it is crucial to have a clean and sustainable technology, which should be easy to implement, more environmental friendly and efficient in treating variety of pollutants in wastewater. Textile wastewater comprises a variety of dyes and pigments, therefore, it becomes essential to promote the prevailing technology and provide new methodologies that degrade the mixture of toxic dyes and pigments rather than individual pigment (Gupta et al. 2015). Photocatalytic degradation is one of the most promising green technologies that can be relied to complete removal of organic dyes and colorants in industrial wastewater without producing any residues and secondary pollutants (Lathasree et al. 2004; Lizama et al. 2002). Titanium dioxide ( $\text{TiO}_2$ ) is a widely used photocatalyst because of its chemical stability, abundance, inoffensiveness, and lot of applications in various fields (Kusvuran et al. 2005; Fuyuki et al. 1988; Kurtz and Gordon 1986; Shivaraju et al. 2016). However, light absorption range of pure  $\text{TiO}_2$  is limited to the ultraviolet (UV) spectrum of light due to its wide bandgap (approximately 3.2 eV). To shift absorption range of  $\text{TiO}_2$  to visible spectrum, various modification approaches such

as surface modification (Li et al. 2009), size optimization (Almquist and Biswas 2002), variation of composition for co-catalyst (Dhumal et al. 2009), and doping (Asahi et al. 2001; Irie et al. 2003; Lee et al. 2015) have been pursued. Among these modification approaches, doping of metal or non-metals into  $\text{TiO}_2$  has proved considerable shifting of absorption range to visible spectrum of light (Kardarian et al. 2016; Priyanka et al. 2016). Doped metals or non-metal ions into  $\text{TiO}_2$  can explain bandgap energy tunings for the visible spectrum of light that emphasizes the utilization of natural sunlight as an alternative driving energy for photocatalyst-based AOPs. There are various advantages in modification of  $\text{TiO}_2$  by doping with non-metals such as narrowing bandgap tuning toward absorbing visible spectrum of light, enhanced impurity energy levels, controlling the shape, size, morphologies, and recombination processes mitigation (Chen et al. 2015; Cheng et al. 2016).

Hence, the aim of this study was to prepare visible light active  $\text{TiO}_2$  polyscales by doping Mg to enhance the photocatalytic degradation efficiencies and its application in the degradation of most commonly used organic dyes and pigments in different industries. Photocatalytic treatment efficiency of Mg-doped  $\text{TiO}_2$  polyscales in real-time textile industrial wastewater under natural sunlight illumination as an alternative and renewable driving energy was also demonstrated for practical applications.

## Materials and methods

### Preparation of Mg-doped $\text{TiO}_2$

Preparation of Mg-doped  $\text{TiO}_2$  polyscales was carried out under mild sol-gel processes using titanium tetra isopropoxide (TTIP) as an initial precursor. During the preparation of Mg-doped  $\text{TiO}_2$ , 10 ml TTIP (Spectrochem, Pvt. Ltd, India) of 98% purity was added into the 25 ml deionized water and 25 ml ethyl alcohol (Changshu Yangyuan Chemical, China) mixture with constant stirring on the magnetic stirrer. About 0.1 mg of magnesium sulphate (SD fine-chem Ltd. India) was dissolved in 1 ml of concentrated  $\text{HNO}_3$  (Merck Pvt. Ltd. India) that gives  $\text{Mg}(\text{NO}_3)_2$  and it was added into the homogeneous mixture dropwise as a source of Mg dopant. The resultant mixture was continuously stirred (350–500 rpm) for 5 h at room temperature and then kept for aging in a dark box without any disturbance for 24 h. Later, the aqueous mixture of Mg-doped  $\text{TiO}_2$  was washed continuously with deionized water and dried in a dust-free hot air oven at 50 °C. Then, the obtained powder was treated in a dust-free muffle furnace using a silica vessel provided with lid at 450 °C for 2 h. Finally, it was quickly quenched to room temperature under a cooling system to obtain desired crystallinity and

active surface morphology. Figure 1 illustrates the schematic preparation of Mg-doped TiO<sub>2</sub> polyscales through sol–gel technique.

### Characterization of Mg-doped TiO<sub>2</sub>

As prepared, Mg-doped TiO<sub>2</sub> polyscales were characterized using different analytical techniques to know obtained properties. The optical and band energy shifting characteristics of Mg-doped TiO<sub>2</sub> polyscales were investigated using UV–visible spectrophotometer (Shimadzu UV-2100) and dilute alcohol was used for suspension of particles. Powder X-ray diffractometer (Hitachi, Model S- 4000, Japan) was used to identify the phase composition and crystalline structures with Bragg's angle ranging from 10° to 70° with a speed of 3° per minute using a nickel-filtered Cu K $\alpha$  radiation source and obtained results were ratified by comparing with JCPDS files (PCPDF Win-2.01). The weight% of Mg and TiO<sub>2</sub> in the final product was determined by XRF spectroscope (Bruker, model S4 pioneer). The structural elucidation and important functional groups in Mg-doped TiO<sub>2</sub> polyscales were investigated by Fourier transform infrared spectroscopy (JASCO-460 PLUS, Japan). Morphology and microstructures of Mg-doped TiO<sub>2</sub> polyscales were scanned by scanning electron microscope (Hitachi, Model S-4000, Japan). Photocatalytic activity of Mg-doped TiO<sub>2</sub> polyscales was determined under the visible light illumination (100 W tungsten bulb,

Philips) using different dyes as model dye solution (Rice et al. 2012).

### Photocatalytic degradation experiment

Photocatalytic degradation of industrial dyes was studied using Mg-doped TiO<sub>2</sub> polyscales under natural sunlight irradiation. Photocatalytic degradation efficiency of Mg doped polyscales was studied using five major dyes such as brilliant blue G 250 (Lobo Chem. India), brilliant green (HiMedia Pvt. Ltd. India), methyl violet 10B (HiMedia Pvt. Ltd. India), methyl red (Merck Pvt. Ltd. India), and methyl orange (HiMedia Pvt. Ltd. India) as model pollutants in aqueous media and these dyes are significantly used in various industries. TiO<sub>2</sub> The dye solutions (0.01 M) were prepared using deionized water. During the photocatalytic degradation experiments, 50 ml of dye solution was taken from the reaction vessel of 100 ml capacity and about 0.5 mg of Mg-doped TiO<sub>2</sub> polyscales were added then exposed to the light source. All the photocatalytic experiments were carried out for 5 h irradiation under natural sunlight of sunny day (From 10.30 am to 3.30 pm). Two sets of control experiment were maintained to each type of dye degradation study without adding photocatalyst under natural sunlight and in dark place without disturbance. Initial, interval, and final concentrations (after 5 h irradiation) of dye stuffs in the aqueous media were determined by spectroscopic methods with respective  $\lambda_{\max}$  of each dye (Rice et al. 2012). All the dye stuffs in the aqueous media were measured using double beam UV–Vis spectrophotometer (Shimadzu UV-2100, Japan). Photocatalytic treatment of real-time textile wastewater using Mg-doped TiO<sub>2</sub> polyscales was assessed by following the same experimental procedure under different light sources. Textile wastewater was collected from a textile industry located at Nanjangudu industrial area in Mysore District and as collected wastewater was diluted to the required concentration in order to allow sunlight penetration without obstacles. Variation in chemical oxygen demand (COD) of textile wastewater was considered as a momentous parameter to determine the photocatalytic degradation efficiency. The photocatalytic treatment of textile wastewater was carried out for 5 h irradiation time initially and likely continued up to 24 h by irradiating under natural sunlight for 6 h in each sunny day (from 10.00 am to 4.00 pm). Photocatalytic degradation efficiency (%) of Mg-doped TiO<sub>2</sub> polyscales in the degradation of industrial dyes and textile wastewater was calculated respectively by following equation.

$$\text{Photodegradation efficiency (\%)} = \frac{C_i - C_f}{C_i} \times 100 \quad (1)$$

where,  $C_i$  is the dye initial concentration and  $C_f$  is the dye final concentration.

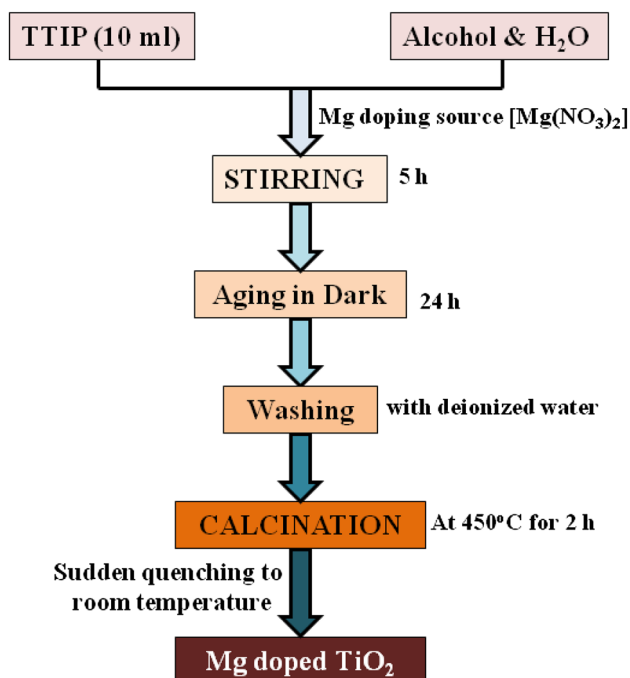


**Fig. 1** Schematic of Mg-doped TiO<sub>2</sub> polyscales preparation under Sol–gel processes

Important factors such as pH, catalyst load, light sources, and dye concentration, which affect on the photocatalytic degradation rate and reusability of Mg-doped TiO<sub>2</sub> polyscales were studied using brilliant dye under natural sunlight for 5 h irradiation time. Recovery of photocatalyst from the aqueous dye solution was carried out by centrifuge method and dried under room conditions.

## Results and discussions

### Characteristics of Mg-doped TiO<sub>2</sub> polyscales

Mg-doped TiO<sub>2</sub> polyscales were synthesized through mild sol–gel process and as prepared photocatalysts were characterized using suitable analytical techniques to know the functionalities obtained under sol–gel processes. The XRF results of Mg-doped TiO<sub>2</sub> was revealed the presence 0.8 wt % of Mg/MgO with TiO<sub>2</sub> (97 wt %), which apparently affect on the band width of TiO<sub>2</sub>. The bandgap energy shifting characteristics of Mg-doped TiO<sub>2</sub> polyscales were investigated using UV–Vis spectrophotometer and the results obtained were compared with pure TiO<sub>2</sub>. The UV–Vis absorption spectrum of Mg-doped TiO<sub>2</sub> polyscales and pure TiO<sub>2</sub> particles are depicted in Fig. 2. The spectrum of Mg-doped TiO<sub>2</sub> polyscales and pure TiO<sub>2</sub> exhibited a strong absorption band at 380–420 and 387 nm that are near UV region, respectively. Mg-doped TiO<sub>2</sub> polyscales showed broad absorption edges at 398 nm, which is in the range of visible spectrum of light. The optical absorption edges of Mg-doped TiO<sub>2</sub> polyscales showed considerably shifted edges toward visible spectrum of light when compared with pure TiO<sub>2</sub>. The shift in the absorption edge to smaller photon energy implies a decreased energy level in the conduction band, and consequent narrowing band gap energy (Asahi et al. 2001; Irie et al. 2003; Ihara et al.

2003). This shifting in the absorption edge towards near-visible region clearly implies band-tuning of Mg-doped TiO<sub>2</sub> polyscales. Mg-doped TiO<sub>2</sub> polyscales confirmed a consequent shifting of bandgap energy from 3.2036 to 3.0955 eV after doping Mg into the TiO<sub>2</sub> crystalline system; it induces the apparent activation of Mg-doped TiO<sub>2</sub> polyscales under natural sunlight illumination that consists of 90 and 10% of visible and UV spectrum of light, respectively.

Powder X-ray diffraction (XRD) patterns were recorded for Mg-doped TiO<sub>2</sub> polyscales and pure TiO<sub>2</sub> in order to determine the crystalline structure and phase compositions. In Fig. 3, spectra (a) and (b) indicate the XRD patterns of Mg-doped TiO<sub>2</sub> particles and pure TiO<sub>2</sub> respectively. XRD pattern of Mg-doped TiO<sub>2</sub> polyscales are dominantly indexed to JCPDS files 84-1285 and 78-2485; it confirmed the mixed phases of anatase (84-1285) and rutile (78-2485) crystal structures (Kohlrausch et al. 2015; Devi and Kavitha 2014; Shivaraju et al. 2010a, b; Harikumar et al. 2013). Dominant peaks of anatase and rutile are sharp and clearly observed particularly at 2θ of 25.2 (101) and 27.2 (110), respectively. Moreover, XRD pattern of Mg-doped TiO<sub>2</sub> polyscales showed the characteristic peak of Mg in TiO<sub>2</sub> crystalline structures (JCPDS: 87-0652) at 2θ of 37.5° (011) and 44° (012) (Lin et al. 2008). It was observed that mixed phases of anatase and rutile were obtained due to the influence of Mg dopant in the formation of TiO<sub>2</sub> crystals. Moreover, the spectrum of Mg-doped TiO<sub>2</sub> polyscales differs from the pure TiO<sub>2</sub>, which is anatase phase and it shows band broadening with decreased peak intensity. Such variations can be attributed to the effect of smaller particle size, which affects the vibrational amplitudes and force constant of nearest neighboring bond (Kaviyarasu and Premanand 2013). However, such smaller particle size along with the mixed phases of anatase and rutile

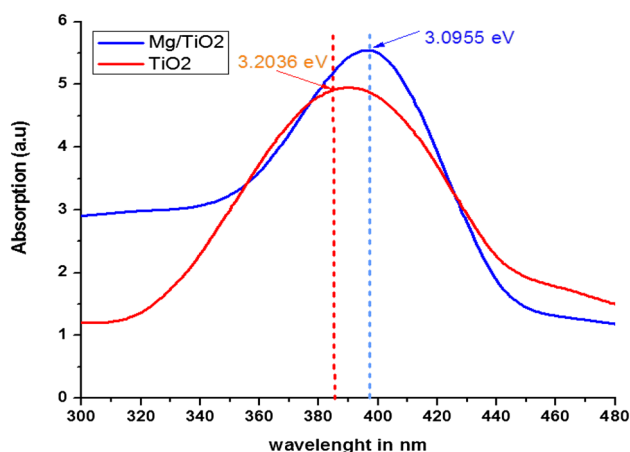


**Fig. 2** Bandgap energy shifting characteristics of pure TiO<sub>2</sub> and Mg-doped TiO<sub>2</sub> polyscales prepared under Sol–gel processes

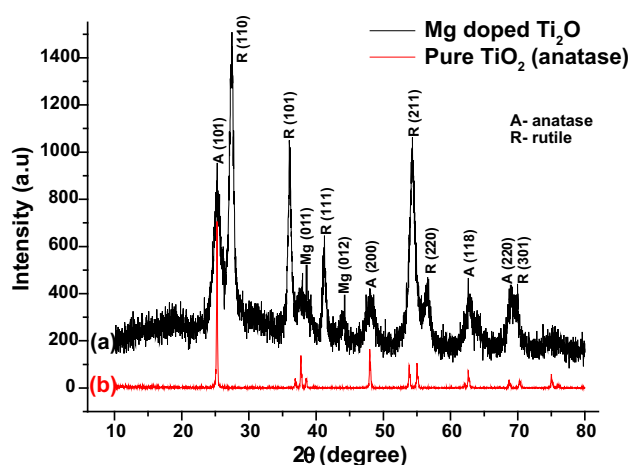


**Fig. 3** Powder X-ray patterns of **a** Mg-doped TiO<sub>2</sub> polyscales prepared under Sol–gel processes; **b** pure TiO<sub>2</sub>

constituents are expected to intensify the photocatalytic reactivity of  $\text{TiO}_2$  under visible light (Kaviyarasu and Premanand 2013; Liu et al. 2011; Truong et al. 2012). The XRD pattern of Mg-doped  $\text{TiO}_2$  polyscales indicated increased peak intensity inducing well crystalline phases, which are apparently stable and enhance the photochemical activities (Devi and Kavitha 2014; Shivaraju et al. 2010a, b; Harikumar et al. 2013).

FTIR spectra of Mg-doped  $\text{TiO}_2$  polyscales and pure  $\text{TiO}_2$  are shown in Fig. 4a, b. FTIR spectra of Mg-doped  $\text{TiO}_2$  polyscales showed comparatively narrow stretching vibration of O–H bond from hydroxyl and O–H bending of molecularly physisorbed moisture at 3417.24 and 1639.3  $\text{cm}^{-1}$ , respectively, than pure  $\text{TiO}_2$ . It clearly indicates a negligible amount of physisorbed moisture in Mg-doped  $\text{TiO}_2$  polyscales (Devi and Kavitha 2014; Shivaraju et al. 2010a, b). A characteristic band with strong and wide absorption at lower energy region ( $<420 \text{ cm}^{-1}$ ) is attributed to the formation of O–Ti–O lattice (Shivaraju et al. 2010a, b). The stretching band corresponding to the magnesium in lattice structure (Ti–Mg–O–Ti) may be identified at lower energy absorption region (426.5  $\text{cm}^{-1}$ ) in the spectrum (Fig. 4b) (Choudhury and Choudhury 2014). FTIR result clearly indicates the presence of Mg/MgO as doping impurities in Mg-doped  $\text{TiO}_2$  photocatalytic system.

The SEM image was used to determine the morphology of Mg-doped  $\text{TiO}_2$  polyscales. The growth of mixed and agglomerated spherical shaped particles of Mg-doped  $\text{TiO}_2$  can be clearly seen in Fig. 5. These SEM images indicate that Mg-doped  $\text{TiO}_2$  polyscales have spherical morphology creating high surface area and porosity, which is quite

suitable for enhancing photocatalytic degradation of organic dyes and pollutants.

The photocatalytic activity of Mg-doped  $\text{TiO}_2$  polyscales was determined using an aqueous dye solution of brilliant green (Himedia, laboratory grade), under both visible light and natural sunlight source (sunny day). Simultaneously, blank experiments were also maintained without adding photocatalyst. The photocatalytic efficiency of Mg-doped  $\text{TiO}_2$  polyscales was compared with undoped  $\text{TiO}_2$  (pure) and Mg-doped  $\text{TiO}_2$  polyscales exhibited efficient photocatalytic activities under both light sources when compared to the pure  $\text{TiO}_2$  and the results obtained can be seen in Fig. 6. Mg-doped  $\text{TiO}_2$  polyscales showed considerable degradation efficiency under natural sunlight (65.6%), which attributed to the band tuning towards visible spectrum by doping of Mg in  $\text{TiO}_2$  structure.

### Photocatalytic degradation of industrial dyes and pigments

Discharge of colored water with varieties of dye substances from industries are the major environmental problems causing water pollution all over the world today (Blanco et al. 2012; Zolinger 1987; Saggiaro et al. 2011; Dave and Dave 2009; Divya et al. 2009; Wijannarong et al. 2013; Gupta et al. 2014; Weber and Adams 1995; Shivaraju et al. 2010a, b). Five different dyes commonly used in the textile and food industries were used for the photocatalytic degradation experiments. Mg-doped  $\text{TiO}_2$  polyscales showed comparatively higher photocatalytic degradation efficiency in the destruction of industrial dyes than pure  $\text{TiO}_2$ . Photocatalytic degradation efficiency of different

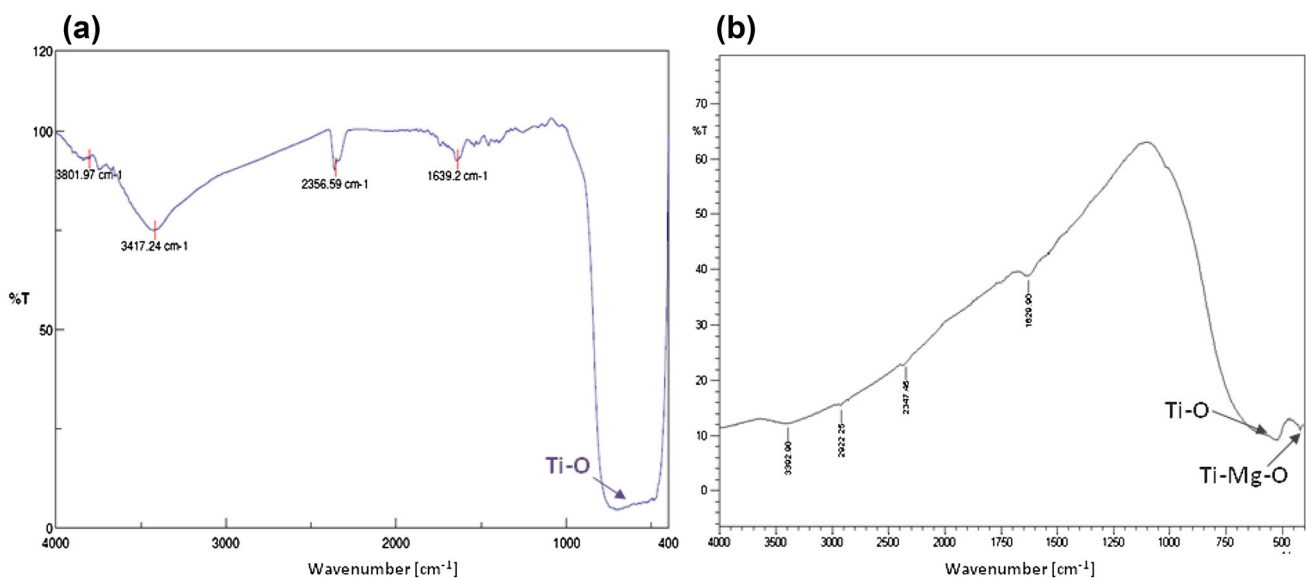


**Fig. 4** FTIR spectra of **a** pure  $\text{TiO}_2$ ; **b** Mg-doped  $\text{TiO}_2$  polyscales prepared under Sol–gel processes



**Fig. 5** SEM images of Mg-doped TiO<sub>2</sub> polyscales prepared under sol-gel processes

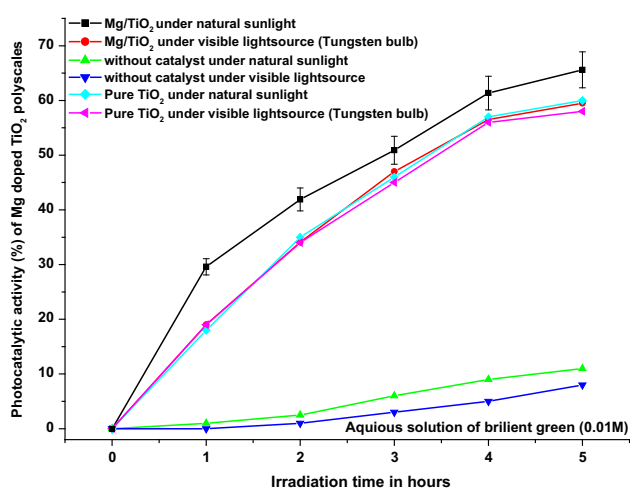
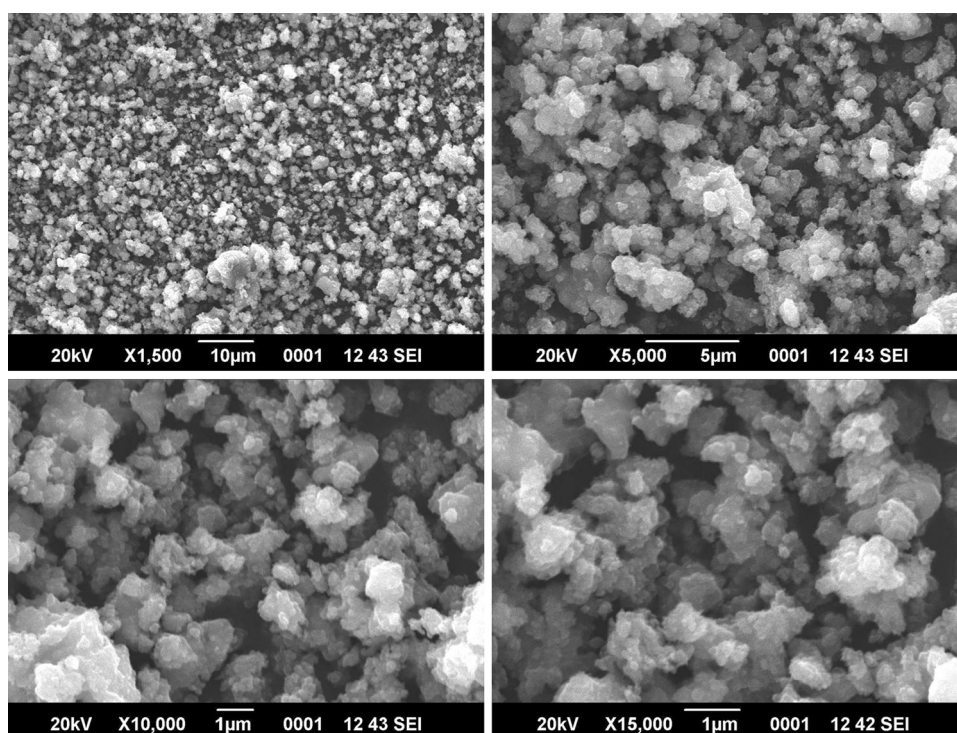


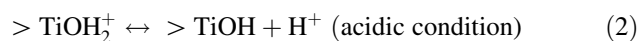
**Fig. 6** Photocatalytic activity of Mg-doped TiO<sub>2</sub> polyscales under visible light sources

organic dyes in aqueous media under natural sunlight as an alternative driving energy is shown in Fig. 7a–f. Results obtained indicate the varied degradation efficiencies for industrial dyes such as methyl violet (100%), methyl red (80%), methyl orange (79%), brilliant green (73%), and brilliant blue (64%) under the same experimental conditions. Of all the five industrial dyes considered for the photocatalytic degradation study, the degradation efficiency for brilliant blue was minimum (Fig. 7a) due to the complexity in molecular structure and strong coloring properties, which obstruct the light penetration in aqueous media.

## Effect of important factors on photocatalytic degradation of industrial dyes

### Effect of initial pH

The photocatalytic degradation efficiency strongly depends upon the *pH* of the aqueous dye solution. The effect of *pH* on photocatalytic degradation rate of brilliant green dye (0.01 M) was assessed using 0.5 mg of catalyst load for 5-h duration under visible light source (Tungsten light-60 W, Philips) by varied *pH* from 2 to 12 adjusted using diluted HNO<sub>3</sub> or NaOH solution. The photocatalytic degradation rate of brilliant green dye was significantly increased up to 100% under the alkaline as well as acidic *pH* and the results obtained can be seen in Fig. 8. Increased rate of photodegradation under alkaline condition can be attributed to the increase of hydroxyl ions, which induces more hydroxyl radicals that can form hydrogen peroxide. This, in turn, gives rise to the hydroxyl radicals. Under acidic condition, the perhydroxyl radicals can form hydrogen peroxide, which gives rise to the hydroxyl radicals. When Mg/TiO<sub>2</sub> contacts the aqueous dye solution, it shows amphoteric nature and the amphoteric surface functionality is the titanol and denoted as >TiOH. The hydroxyl group on the TiO<sub>2</sub> surface undergoes the following acid–base equilibrium (Eqs. 2, 3):



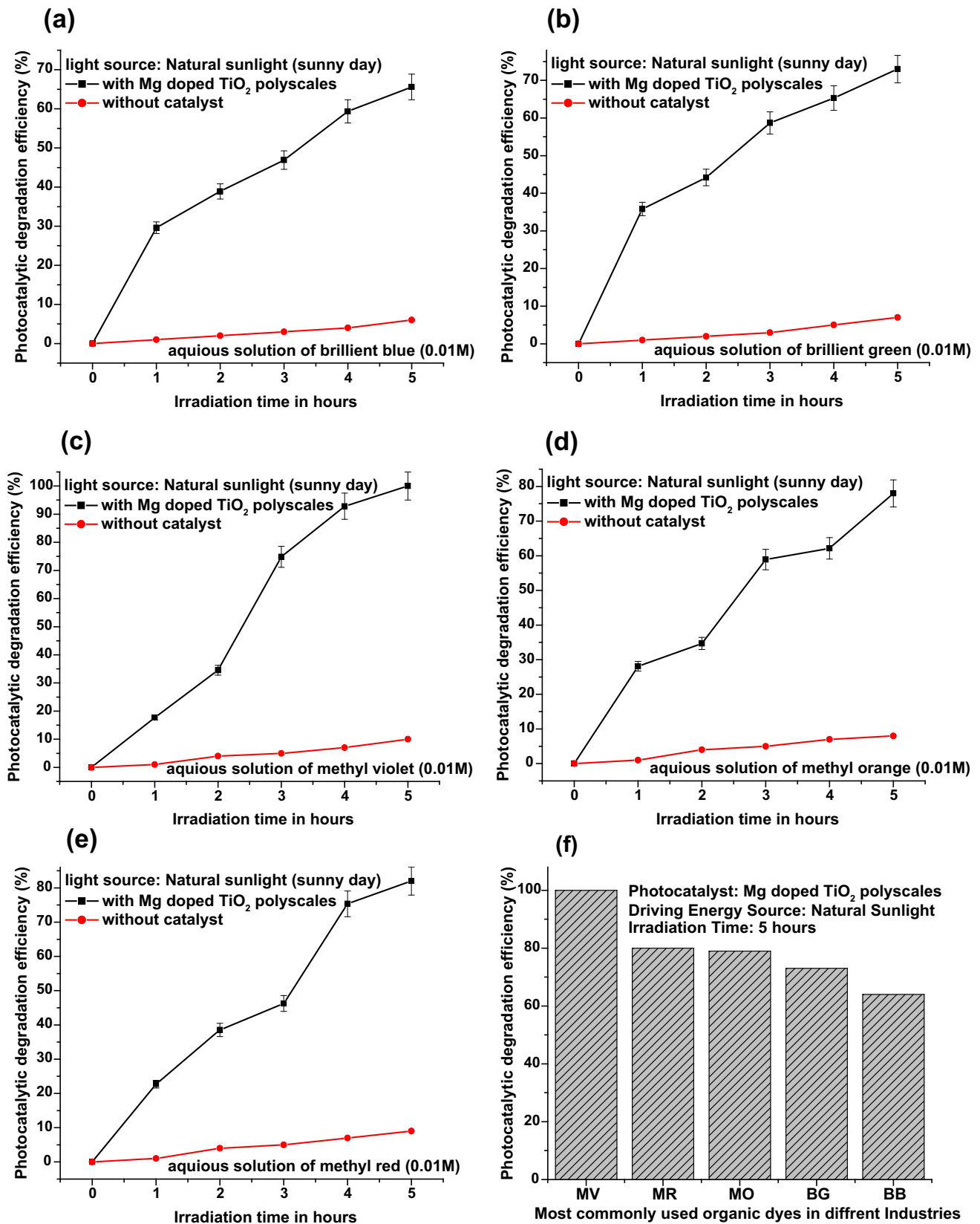


**Fig. 7** Photocatalytic destruction efficiencies of Mg-doped TiO<sub>2</sub> polyscales in the degradation of **a** Brilliant blue G 250; **b** Brilliant green; **c** Methyl violet 10B; **d** Methyl red; **e** Methyl orange; **f** comparison of individual dye degradation level by Mg-doped TiO<sub>2</sub> polyscales

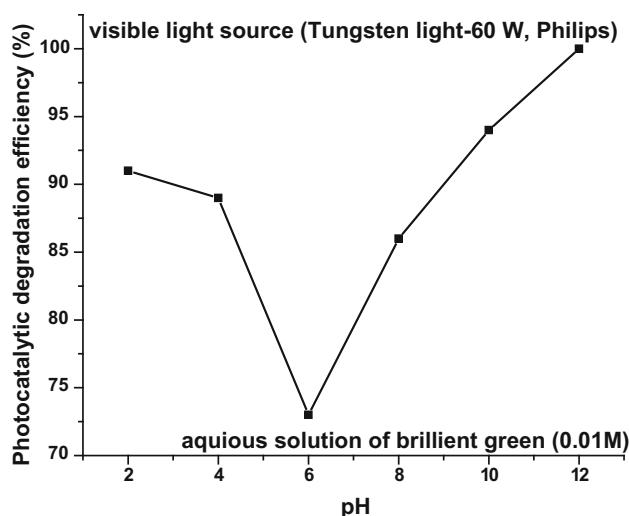
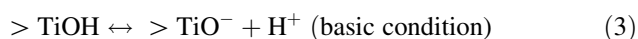


**Fig. 8** Effect of initial pH on photocatalytic degradation efficiency



Below the neutral *pH*, the Mg/TiO<sub>2</sub> surface is positively charged and above this neutral *pH* the Mg/TiO<sub>2</sub> surface is negatively charged. In particular, for organic compounds that undergo photoreaction, the variations in the *pH* not only influence the quantity of organic substrate, but also surface properties of the photocatalysts. In addition, the band edge energy of Mg/TiO<sub>2</sub> will change with *pH* and, thermodynamically, this change would lead to a change in photocatalytic degradation efficiency. In this regard, the *pH* would greatly influence the photocatalytic degradation rate of industrial dyes and thus an increase or decrease in *pH* from neutral *pH* value the rate of photocatalytic reaction will be increased.

### Effect of photocatalyst load

The photocatalytic degradation efficiency is based on photocatalyst load and photocatalyst load largely depends on the nature of the catalysts. The photocatalytic degradation study of brilliant green dye was carried under varied catalyst loads. When the photocatalyst load was varied from 0.1 to 1.0 mg, it was observed that the degradation rate of dye was significantly increased up to 73% at the amount of 0.6 mg of catalyst load and the results obtained can be seen in Fig. 9. The results obtained showed increased degradation with an increased amount of catalyst load until a saturation value of 0.6 mg. The degradation efficiency was not significantly enhanced beyond 0.6 mg of catalyst load, due to increased numbers of available active sites on the surface of catalyst for the photoreaction, which in turn increases the rate of radical formation in aqueous solution. It showed a drastic reduction of degradation rate in the range of 0.1–0.5 mg/50 ml, which is attributed to the

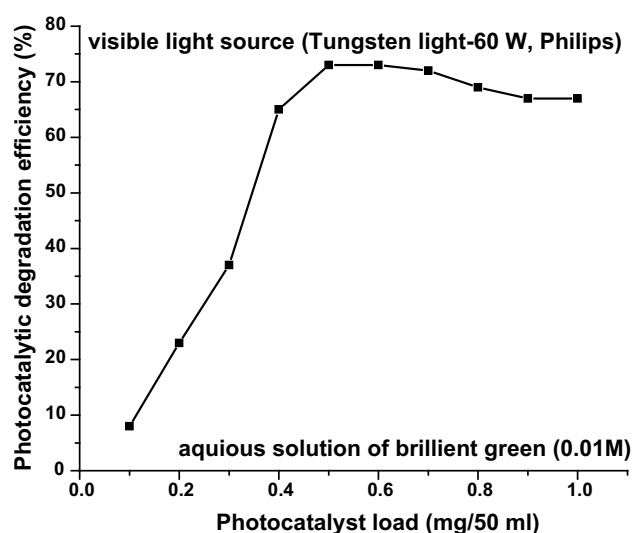


**Fig. 9** Effect of photocatalyst load on photocatalytic degradation efficiency

lack of active sites for photo-degradation of dye molecules. The photo-degradation rate was slightly reduced beyond the amount of catalysts load at 0.6 mg/50 ml; this could be attributed to the large amount of catalyst particles in the solution, which leads to light scattering and reduction in light penetration through the aqueous medium by decrease in transparency of aqueous dye solution.

### Effect of initial dye concentration

The effect of initial concentration of brilliant green dye in an aqueous solution on the photocatalytic degradation efficiency was studied under varied dye concentrations. The concentration of brilliant green dye was varied from 0.01 to 0.12 M in the aqueous solution. The photo-degradation rate of brilliant green dye decreased with an increased concentration of dye in the aqueous solution (Fig. 10). When concentration of dye was decreased in the aqueous solution, it became more transparent and clear from intense colour and the path length of photons entering into that solution increased. When photons easily reached the photocatalyst surface in the aqueous medium, the production of hydroxyl and superoxide radicals increased, and it apparently induced the photo-degradation efficiency of industrial dye molecules in the aqueous solution.

### Effect of light sources

The effect of light sources on photo-degradation efficiency of brilliant green dye was studied under different light sources. A set of experiments was carried out in a dark chamber to study the importance of light for the activation of the photocatalyst. All the photocatalytic experiments



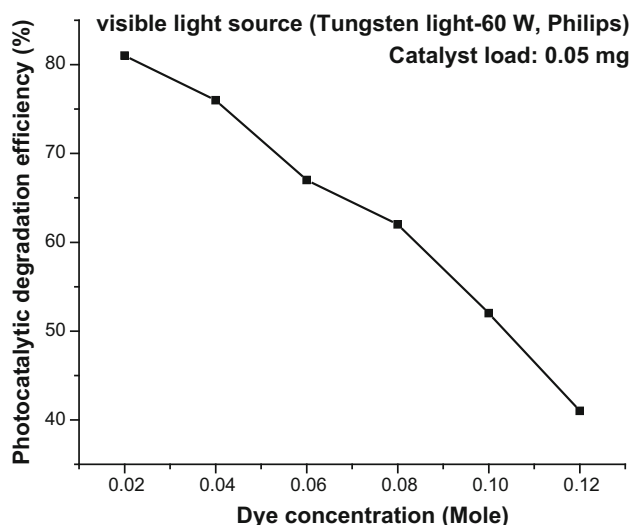


**Fig. 10** Effect of initial dye concentration on photocatalytic degradation efficiency

were conducted under the same experimental conditions such as constant temperature (room temperature), photocatalyst load, pH and dye concentration. Light sources like UV light source (16 W, Philips) and visible light sources such as tungsten light (60 W, Philips), LED light (16 W, Everyday) and natural sunlight were used for the photocatalytic degradation study. The effects of light sources on photocatalytic degradation efficiency can be seen in Fig. 11. Highest degradation efficiency was observed under the LED light (90%) and tungsten light sources (87%) when compared to UV light source (71%). Under darkness, the degradation rate of dye was very poor due to the lack of photon energy for the activation of photocatalysts. The photocatalytic degradation rate of brilliant green dye in the

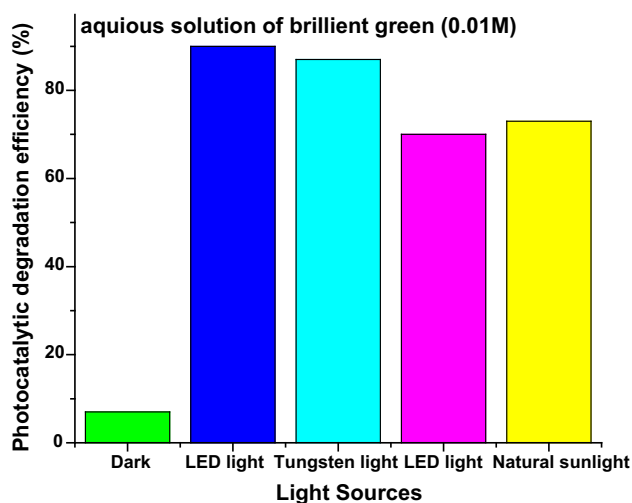


**Fig. 11** Effect of light sources on photocatalytic degradation efficiency

aqueous solution under natural sunlight was also nearest to the LED and tungsten light sources. Without light source degradation efficiency was neglected, because, without light, photoelectron and photohole generation or recombination will not occur on the photocatalyst.

### Photocatalytic treatment of real-time textile effluent

Photocatalytic degradation of dyes and other organic pollutants in the real-time textile effluent was studied using Mg-doped  $\text{TiO}_2$  polyscales under natural sunlight illumination as an alternative and renewable driving energy source that attributes the sustainable treatment of industrial wastewater. Mg-doped  $\text{TiO}_2$  polyscales showed comparatively higher efficiency in the degradation of organic dyes and pollutants in the textile wastewater and results obtained can be seen in Fig. 12. Photocatalytic degradation of textile wastewater showed 64.55% (COD reduced from 1692 to 600 mg/l) degradation of organic dyes and pollutants within 6-h duration by utilizing sunlight. Up to 92% degradation (COD reduced to 135.36 mg/l) was achieved within 24 h under solar light irradiation. Therefore, utilization of widely available solar energy as an alternative driving energy for wastewater treatment could be one of the most sustainable ways of industrial wastewater reclamation. Moreover, the research revealed that Mg-doped  $\text{TiO}_2$  polyscales showed comparatively higher degradation efficiency in the model aqueous dye solution than the real-time textile wastewater. It could be attributed to the fact that other contaminants may reduce the photocatalytic activities by reduction of the irradiation rate through obstructing the light waves to

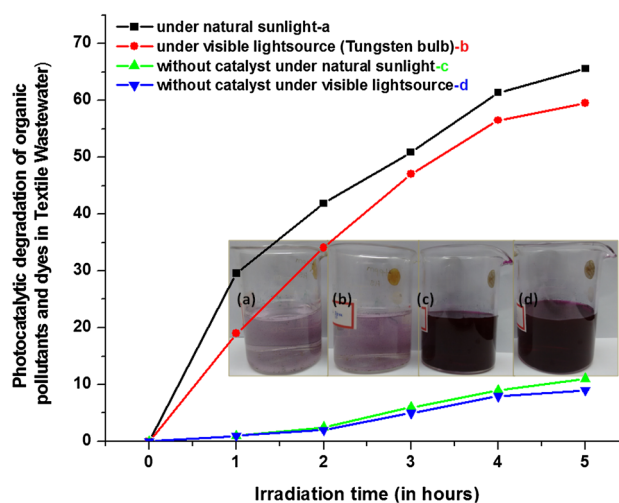


**Fig. 12** Photocatalytic treatment of textile wastewater using Mg-doped  $\text{TiO}_2$  polyscales under natural sunlight

reach the surface of photocatalyst. The reduction of COD level in the wastewater confirmed the photocatalytic degradation of dyes and colorants along with other organic pollutants in the textile wastewater. Apparently, Mg-doped TiO<sub>2</sub> polyscales can be utilized as excellent photocatalysts by harvesting the natural sunlight as a renewable and potential alternative driving energy for the treatment of industrial wastewater. In addition, the present research revealed that recovery of suspended photocatalytic particles from aqueous media was quite difficult and further it can be effectively dealt by suspension of suitable supporting materials (Shivaraju et al. 2010a, b; Shivaraju 2011), which are decorated with Mg-doped TiO<sub>2</sub> polyscales in aqueous media. Efficiency of supported Mg-doped TiO<sub>2</sub> polyscales could be attributed to the continuous and ease recovery of photocatalyst after industrial wastewater and the animated photocatalytic treatment processes of textile wastewater can be seen in the Appendix A. Supplementary materials.

### Reusability study

Reusability of Mg-doped TiO<sub>2</sub> polyscales was studied using brilliant dye under natural sunlight for 5 h irradiation time. As-regenerated Mg-doped TiO<sub>2</sub> polyscales was studied for their reusability for the degradation of dye molecules and the results obtained showed decreased efficiency of regenerated Mg-doped TiO<sub>2</sub> polyscales after 2–3 usage cycles. The decreased efficiency of recycled catalysts attributed to the blocking of active pores by dye molecules which apparently reduces the photocatalytic activities of Mg-doped TiO<sub>2</sub> polyscales and the results can be seen in Fig. 13.

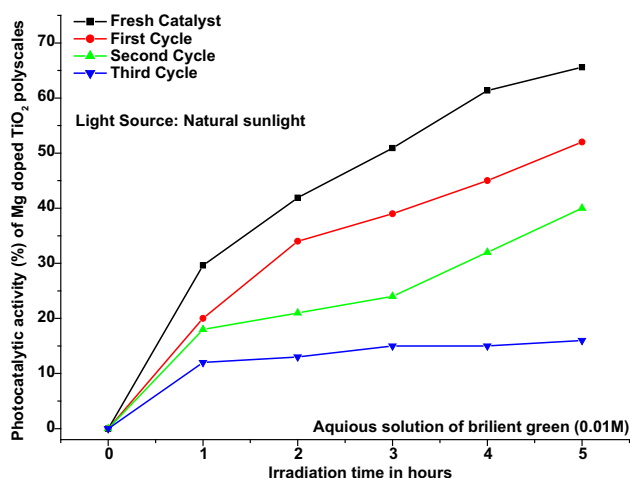


**Fig. 13** Reusability efficiency of Mg-doped TiO<sub>2</sub> polyscales under natural sunlight

### Conclusion

The present research presented the preparation of the visible-light responsive Mg-doped TiO<sub>2</sub> polyscales through mild sol-gel technique. The characterization results revealed that well crystalline phases of anatase and rutile, stable and smaller polyscales, desired structural elucidation and morphology, considerable shifting and narrowing of bandgap energy, and higher photocatalytic activities in Mg-doped TiO<sub>2</sub> polyscales. Moreover, Mg-doped TiO<sub>2</sub> polyscales confirmed the excellent degradation efficiency of several organic dyes and colorants, which are commonly used in the textile and food industries under natural sunlight as a renewable and alternative energy source. Mg-doped TiO<sub>2</sub> polyscales assisted wastewater treatment technique with suitable alteration in the functionalities of the photocatalyst. The incorporation of the polyscales fabricated in suitable supporting materials might be substituted with the conventional treatment methods in the removal of toxic organic dyes and other organic pollutants in the industrial wastewater by harvesting the alternative and sustainable energy in natural sunlight.

**Acknowledgements** The authors thank Prof. R. Somashekar, University of Mysore, and Dr. B. M. Gurupadaya, JSS University, Mysore, for providing XRD and FTIR facilities, respectively, in the research work. The authors would also like to thank STIC, Cochin University of Science & Technology, Cochin, for providing SEM facilities. The authors thank the Head, Dr. S. Suriyanarayanan, Department of Water and Health, JSS University, for providing necessary suggestions and research facilities.

**Open Access** This article is distributed under the terms of the Creative Commons Attribution 4.0 International License (<http://creativecommons.org/licenses/by/4.0/>), which permits unrestricted use, distribution, and reproduction in any medium, provided you give appropriate credit to the original author(s) and the source, provide a link to the Creative Commons license, and indicate if changes were made.

### References

- Almquist CB, Biswas P (2002) Role of synthesis method and particle size of nanostructured TiO<sub>2</sub> on its photoactivity. *J Catal* 212(2):145–156
- Asahi R, Morikawa T, Ohwaki T, Aoki K, Taga Y (2001) Visible-light photocatalysis in nitrogen-doped titanium oxides. *Science* 293(5528):269–271
- Behzad S, Mahin N, Afshin M (2012) Hydrothermal synthesis of surface-modified, manganese-doped TiO<sub>2</sub> nanoparticles for photodegradation of methylene blue. *Environ Eng Sci* 29:1032–1037
- Blanco J, Torrades F, Varga M, Montano JG (2012) Fenton and biological-Fenton coupled processes for textile wastewater treatment and reuse. *Desalination* 286:394–399
- Chen D, Chen S, Quan H, Huang Z, Lu L, Luo X, Guo L (2015) Synergetic effects of W<sup>6+</sup> doping and Au modification on the photocatalytic performance of mesoporous TiO<sub>2</sub> clusters. *Adv Powder Technol* 26(6):1590–1596

- Cheng Y, Zhang M, Yao G, Yang L, Tao J, Gong Z, He G, Sun Z (2016) Band gap manipulation of cerium doping TiO<sub>2</sub> nanopowders by hydrothermal method. *J Alloys Compd* 662:179–184
- Choudhury B, Choudhury A (2014) Microstructural, optical and magnetic properties study of nanocrystalline MgO. *Mater Res Express* 1(2):25026–25031
- CPCB (2009) Status of water supply, wastewater generation and treatment in Class I cities and Class II towns of India, India, pp 10
- Dave SR, Dave RH (2009) Isolation and characterization of *Bacillus thuringiensis* for Acid red 119 dye decolourisation. *Bioresour Technol* 100(1):249–253
- Devi LG, Kavitha R (2014) Review on modified N-TiO<sub>2</sub> for green energy applications under UV/visible light: selected results and reaction mechanisms. *RSC Adv* 4:28265–28299
- Dhumal SY, Daulton TL, Jiang J, Khomami B, Biswas P (2009) Synthesis of visible light-active nanostructured TiO<sub>x</sub> (x < 2) photocatalysts in a flame aerosol reactor. *Appl Catal B* 86(3–4):145–151
- Divya N, Bansal A, Jana AK (2009) Degradation of acidic Orange G dye using UV–H<sub>2</sub>O<sub>2</sub> in batch photoreactor. *Int J Biol Chem Sci* 3(1):54–62
- Divya N, Bansal A, Jana AK (2013) Photocatalytic degradation of azo dye Orange II in aqueous solutions using copper-impregnated titania. *Int J Environ Sci Technol* 10(6):1265–1274
- Firmino PIM, Silva MER, Cervantes FJ, Santos ABD (2010) Colour removal of dyes from synthetic and real textile wastewaters in one- and two-stage anaerobic systems. *Bioresour Technol* 101(20):7773–7779
- Fuyuki T, Kobayashi T, Matsuyama H (1988) Effects of small amount of water on physical and electrical properties of TiO<sub>2</sub> films deposited by CVD method solid-state science and technology—technical notes. *J Electrochem Soc* 135(1):248–250
- Gupta VK, Pathania D, Singh P, Rathore BS (2014) Development of guar gum based cerium(IV) tungstate nanocomposite material for remediation of basic dye from water. *Carbohydr Polym* 101:684–691
- Gupta VK, Khamparia S, Tyagi I, Jaspal D, Malviya A (2015) Decolorization of mixture of dyes: a critical review. *Global J Environ Sci Manag* 1(1):71–94
- Harikumar PS, Joseph L, Dhanya A (2013) Photocatalytic degradation of textile dyes by hydrogel supported titanium dioxide nanoparticles. *J Environ Eng Ecol Sci*. doi:10.7243/2050-1323-2-2
- Hassani AH, Seif S, Javid AH, Borghei M (2008) Comparison of adsorption process by GAC with novel formulation of coagulation flocculation for color removal of textile wastewater. *Int J Environ Res* 2(3):239–248
- Ihara T, Miyoshi M, Triyama Y, Marsumato O, Sugihara S (2003) Visible-light-active titanium oxide photocatalyst realized by an oxygen-deficient structure and by nitrogen doping. *Appl Catal B* 42:403–409
- Irie H, Wanatabe Y, Hashimoto KJ (2003) Nitrogen-concentration dependence on photocatalytic activity of TiO<sub>2-x</sub> Nx powders. *Phys Chem B* 107(23):5483–5486
- Kardarian K, Nunes D, Sberna PM, Ginsburg A, Keller DA, Pinto JV, Deuermeier J, Anderson AY, Zaban A, Martins R, Fortunato E (2016) Effect of Mg doping on Cu<sub>2</sub>O thin films and their behavior on the TiO<sub>2</sub>/Cu<sub>2</sub>O heterojunction solar cells. *Sol Energy Mater Sol Cells* 147:27–36
- Kaviyarasu K, Premanand D (2013) Synthesis of Mg doped TiO<sub>2</sub> nanocrystals prepared by wet-chemical method: optical and microscopic studies. *Int J Nanosci* 12(4):1–6
- Khataee AR, Vafaei F, Jannatkah M (2013) Biosorption of three textile dyes from contaminated water by filamentous green algal *Spirogyra* sp.: kinetic, isotherm and thermodynamic studies. *Int Biodeterior Biodegrad* 83:33–40
- Kohlrausch EC, Zapata MJM, Gonçalves RV, Khan S, Vaz MO, Dupont J, Teixeira SR, Santos MJL (2015) Polymorphic phase study on nitrogen-doped TiO<sub>2</sub> nanoparticles: effect on oxygen site occupancy, dye sensitized solar cells efficiency and hydrogen production. *RSC Adv* 123:101276–101286
- Kurtz SR, Gordon RG (1986) Chemical vapour deposition of titanium nitride at low temperatures. *Thin Solid Films* 140(2):277–290
- Kusvuran E, Samil A, Atanur OM, Erbatur O (2005) Photocatalytic degradation kinetics of di- and tri-substituted phenolic compounds in aqueous solution by TiO<sub>2</sub>/UV. *Appl Catal B* 58(3–4):211–216
- Lathasree S, Nageswara R, Sivasankar B, Sadasivam V, Rengaraj K (2004) Heterogeneous photocatalytic mineralisation of phenols in aqueous solutions. *J Mol Catal A: Chem* 223(1–2):101–105
- Lee H, Park YK, Kim SJ, Kim BH, Jung SC (2015) Titanium dioxide modification with cobalt oxide nanoparticles for photocatalysis. *J Ind Eng Chem* 32:259–263
- Li L, Liu J, Su Y, Li G, Chen X, Qiu X, Yan T (2009) Surface doping for photocatalytic purposes: relations between particle size, surface modifications, and photoactivity of SnO<sub>2</sub>:Zn<sup>2+</sup> nanocrystals. *Nanotechnology* 20(15):155706
- Lin PC, Huang CW, Hsiao CT, Teng HS (2008) Magnesium hydroxide extracted from a magnesium-rich mineral for CO<sub>2</sub> sequestration in a gas-solid system. *Environ Sci Technol* 42(8):2748–2752
- Liu JY, Garg B, Ling YC (2011) Cu<sub>x</sub>Ag<sub>y</sub>In<sub>z</sub>Zn<sub>n</sub>Sm solid solutions customized with RuO<sub>2</sub> or Rh<sub>1.32</sub>Cr<sub>0.66</sub>O<sub>3</sub> co-catalyst display visible light-driven catalytic activity for CO<sub>2</sub> reduction to CH<sub>3</sub>OH. *Green Chem* 13:2029–2031
- Lizama C, Freer J, Baeza J, Mansilla HD (2002) Optimized photodegradation of Reactive Blue 19 on TiO<sub>2</sub> and ZnO suspensions. *Catal Today* 76(2–4):235–246
- Maleki A, Shahmoradi B (2012) Solar degradation of Direct Blue 71 using surface modified iron doped ZnO hybrid nanomaterials. *Water Sci Technol* 65(11):1923–1928
- Mohamed RM, Mkhallid IA, Baeissa ES, Al-Rayyani MA (2012) Photocatalytic degradation of methylene blue by Fe/ZnO/SiO<sub>2</sub> nanoparticles under visiblelight. *J Nanotechnol*. doi:10.1155/2012/329082
- Nordin N, Amir SFM, Riyanto Othman MR (2013) Textile industries wastewater treatment by electrochemical oxidation technique using metal plate. *Int J Electrochem Sci* 8:11403–11415
- Polak J, Wilkolazka AJ, Ciesielska AS, Wlizo K, Kopycinska M, Ledakowicz JS, Olczyk JL (2016) Toxicity and dyeing properties of dyes obtained through laccase-mediated synthesis. *J Clean Prod* 112(5):4265–4272
- Priyanka KP, Revathy VR, Rosmin P, Thrivedu B, Elsa KM, Nimmymol J, Balakrishna KM, Varghese T (2016) Influence of La doping on structural and optical properties of TiO<sub>2</sub> nanocrystals. *Mater Charact* 113:144–151
- Qu X, Alvarez PJJ, Li Q (2013) Applications of nanotechnology in water and wastewater treatment. *Water Res* 47(12):3931–3946
- Rice EW, Baird RB, Eaton AD, Clesceri LS (2012) APHA, standard methods for examination of water and wastewater, 22nd edn. American Public Health Association, Washington, DC
- Saggiaro EM, Oliveira AS, Pavesi T, Maia CG, Ferreira LFF, Moreira JC (2011) Use of titanium dioxide photocatalysis on the remediation of model textile wastewaters containing azo dyes. *Molecules* 16(12):10370–10386
- Shivaraju HP (2011) Hydrothermal preparation of novel photocatalytic composite, TiO<sub>2</sub> deposited calcium aluminosilicate beads and their photocatalytic applications. *Integr Publ Assoc* 1(7):1476–1491

- Shivaraju HP, Byrappa K, Vijay Kumar TMS, Ranganathaiah C (2010a) Hydrothermal synthesis and characterization of TiO<sub>2</sub> nanostructures on the ceramic support and their photo-catalysis performance. *Bull Catal Soc Ind* 9:37–50
- Shivaraju HP, Sajan CP, Rungnapa T, Kumar V, Ranganathaiah C, Byrappa K (2010b) Photocatalytic treatment of organic pollutants in textile effluent using hydrothermally prepared photocatalytic composite. *Mater Res Innov* 14(1):80–86
- Shivaraju HP, Muzakkira N, Shahmoradi B (2016) Photocatalytic treatment of oil and grease spills in wastewater using coated N-doped TiO<sub>2</sub> polyscales under sunlight as an alternative driving energy. *Int J Environ Sci Technol* 13:2293–2302
- Truong QD, Le TH, Liu JY, Chung CC, Ling YC (2012) Synthesis of TiO<sub>2</sub> nanoparticles using titanium oxalate complex towards visible light-driven photocatalytic reduction of CO<sub>2</sub> to CH<sub>3</sub>OH. *Appl Catal A* 437:28–35
- Wang MX, Zhang QL, Yao SJ (2015) A novel biosorbent formed of marine-derived *Penicillium janthinellum* mycelial pellets for removing dyes from dye-containing wastewater. *Chem Eng J* 259:837–844
- Weber EJ, Adams RL (1995) Chemical and sediment mediated reduction of the azo dye Disperse Blue 79. *Environ Sci Technol* 29(5):1163–1170
- Wijannarong S, Aroonsrimorakot S, Thavipoke P, Sangjan S (2013) Removal of reactive dyes from textile dyeing industrial effluent by ozonation process. *APCBEE Proc* 5:279–282
- Zolinger H (1987) *Colour chemistry—synthesis, properties of organic dyes and pigments*. VCH Publishers, New York, p 92